ISSN 2349-4506
Impact Factor: 2.265

Global Journal of Engineering Science and Research Management

INVESTIGATION OF FLUTTER BY TWO NUMERICAL SIMULATIONS ANALYSIS FOR SUSPENSION BRIDGES

Ahmed Abdel-Aziz*[1] Walid A. Attia[2]

1* PhD Student in Cairo University and Assistant Lecturer, Civil Eng. Dept., Higher Technological Institute, 6 October, Egypt.

[2] Professor of theory of Structure, Cairo University, Giza, Egypt.

KEYWORDS: Computational fluid dynamics, Discrete vortex method, Critical flutter wind speed, Flutter derivatives, Suspension bridge, Bridge aeroelasticity

ABSTRACT

This paper introduces two methods for calculating the critical wind speed of flutter for Great Belt East Bridge. The first method is the Computational Fluid Dynamics (CFD) by secondary development of Ansys Fluent 14.5, establishing two-dimensional bending and torsional fluid-structure interaction (FSI) numerical model. The second method, is Discrete Vortex Method (DVM) to get flutter derivatives by forced-motion for two cases, the first using only the traditional derivatives A_i and H_i for i=1-3 and the second including the two derivatives, A_4* and H_4*.

Additionally, a realizable (κ-ε) model with enhanced wall treatment turbulence model has been considered to verify its performance in bridge aerodynamics problems. Modal analysis is also carried out to calculate the natural frequencies. It has been found that static aerodynamic coefficients have been correctly modeled using a steady simulations, while the flutter critical wind speed is judged from the time history of unsteady simulations for stationary deck sections. The validity of the simulation methods were verified by comparison of the simulation results with the work done by other researchers and it found that the results are in good agreement.

INTRODUCTION

Wind load is one of the most important design loads in civil engineering structures, especially for long span bridges with low damping and high flexibility. Deck sections of long span bridges are one type of bluff bodies that are usually elongated with sharp corners that make the flow around them to cause aerodynamic instabilities. Such instabilities may cause serious catastrophic structural failure such as, the Old Tacoma Narrows Bridge collapse in 1940. Suspension bridges not only must be designed to support the static wind forces like lift, drag and moment created by the mean wind, but also the dynamic loads created by an interaction between the wind forces and structural motions which is known as aeroelasticity. Deck models are used in wind tunnel tests to obtain aerodynamic and aeroelastic information. However, with computer technology and computational fluid dynamics (CFD) evolution, a lot of these models can also be analyzed by numerical simulations. Flutter occurs due to a structure and wind interaction where the wind speed has passed the critical speed of flutter and negative damping develops [1]. If the structure is experiencing oscillation a positive damping will slowly decrease the amplitude of displacement, on the other hand flutter increases the amplitude of the oscillation as time continues [2].Fig. 1 shows a sinusoidal representation of both positive and negative damping phenomena.

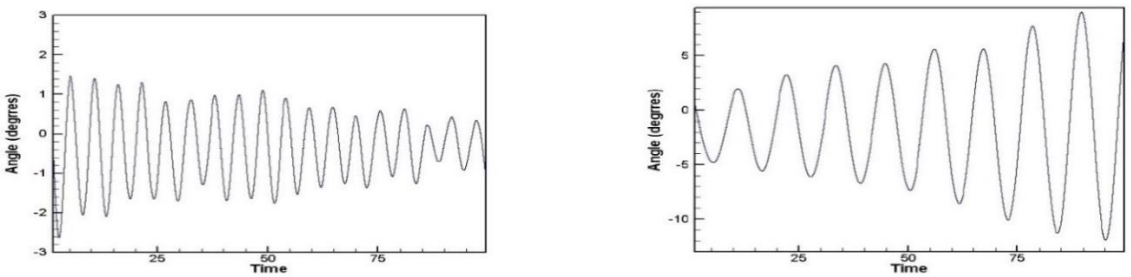

(a) Positive damping (b) Negative damping

Fig. 1 Example of positive and negative damping [2]

The objective of the flutter analysis is to evaluate the lowest critical flutter wind velocity as well as the corresponding flutter frequency .In general, flutter analysis can be conducted in either frequency domain or time

domain .Great achievements have been made in this field based on the long term collaboration of the bridge engineers and the aerodynamic scientists .Several methods have been proposed for flutter analysis of bridges ,such as the full-order flutter analysis method [3], the multimode flutter analysis technique [4], etc. The full-order method is not based on the structural modal but on the system model of the interaction between the structures and aerodynamic forces, meanwhile, the overall influences of structural modal without modal analysis is considered in advance.

Galloping, vortex shedding vibrations, and flutter are the most aeroelastic phenomena that can be seen in long span suspension bridges. Only the last phenomenon will be studied in the present work and will be focused on producing reliable results by establishing a finite element model (FEM) of the Great Belt East Bridge by ANSYS 14.5 to calculate the critical wind speed of flutter. The flutter analysis of the bridge is conducted using the full-order method to provide theoretical reference for flutter analysis of suspension bridges and determining whether the (FE) can lead to a reduction in the number of expensive physical model tests.

METHODOLOGY

Numerical Simulation Principle

Due to the lack of available modules, ANSYS cannot be directly used for flutter analysis. Some efforts should be made [5].In this work, Flutter analysis is accomplished in two different ways:

1) Direct method "Computational fluid dynamics (CFD) based on fluid-structure interaction (FSI)" presented by Selvam [6].
2) Flutter derivative introduced by Simiu and Scanlan [7].

Both methods are based on the observation of the structural response for the cross section rotations of various wind velocity values.

Direct Method

The structure is regarded as a mass, spring and damping system. A schematic diagram of numerical simulation is shown in Fig.2.Fluid control equations for incompressible flow are equations (1) and (2) which represent the continuity and the Navier-Stokes Equation respectively. The first step to ascertain the aerodynamic response of the bridge deck is computation of the aerodynamic force coefficients (C_d,C_l,C_m).After getting these coefficients, drag force, lift force, and moment, can be easily calculated by equations (3), (4) and (5). Fig. 3 shows the sign criteria for the aerodynamic forces. Equations (6) and (7) are the governing structural equations for the heaving and torsional mode respectively.

$$\nabla . V^{-} = 0 \quad (1)$$

$$\frac{\partial V^{-}}{\partial t} + (V^{-} . \nabla) V^{-} = -\frac{1}{\rho}\nabla p + \mu \nabla^2 V^{-} \quad (2)$$

$$F_D = 0.5 \rho U^2 B C_d \quad (3)$$

$$F_L = 0.5 \rho U^2 B C_l \quad (4)$$

$$M = 0.5 \rho U^2 B^2 C_m \quad (5)$$

$$m\ddot{h}(t) + C_h \dot{h}(t) + K_h h(t) = F_L(t) \quad (6)$$

$$I\ddot{\alpha}(t) + C_\alpha \dot{\alpha}(t) + K_\alpha \alpha(t) = M(t) \quad (7)$$

ISSN 2349-4506
Impact Factor: 2.265

Global Journal of Engineering Science and Research Management

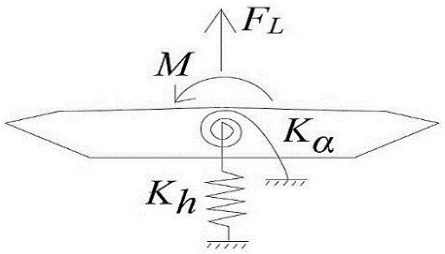

Fig. 2: Schematic diagram of numerical simulation

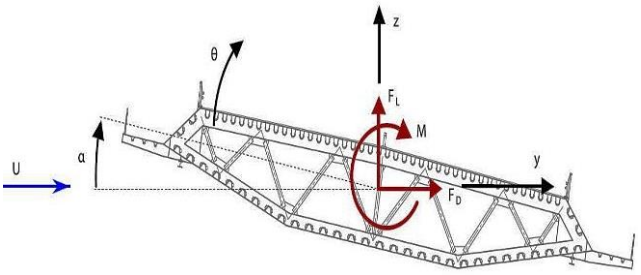

Fig. 3: Sign criteria for the aerodynamic forces [8].

Where:

V, p, t: Velocity, pressure, time respectively.

ρ : Air density.

μ : Air dynamic viscosity.

F_D, F_L, M: Drag force, lift force, and moment respectively.

C_d, C_l, C_m: Coefficients of drag force, lift force, and moment respectively.

U: Reference velocity.

B: Bridge width.

m: Deck mass per unit length.

I: Mass moment of inertia about shear center per unit length.

C_h, C_α: Structural damping coefficients.

K_h, K_α: Translational and rotational spring stiffness.

$\ddot{h}(t)$, $\dot{h}(t)$, $h(t)$: Instantaneous bending acceleration, velocity and displacement respectively.

$\ddot{\alpha}(t)$, $\dot{\alpha}(t)$, $\alpha(t)$: Instantaneous torsional acceleration, velocity and displacement respectively.

The critical velocity for bridges is calculated using FSI. The aeroelastic stability is observed from the free motion of the bridge deck for various wind speeds. The procedure of FSI simulation in every wind speed is shown in Fig.4.

Before calculating the time step, the preliminary value of bending and torsional acceleration, velocity, and displacement are set to be zero [5, 6].For every time step the pressure and velocity are computed around the bridge deck for the given position by solving the continuity and Navier-Stokes Equation as equations (1) and (2).Then the aerodynamic force coefficients acting on the bridge deck are calculated by using equations (4) to (6). This can be done by Fluent [10, 11].

Lift pressure force and moment are represented by the force in y-direction and the force that causes rotation respectively. Lift force is applied at the center of gravity and the moment is applied at the shear center, then the lift and moment are extracted into structural dynamic equations (6) and (7). Then they are solved by using the Newmark-β method to get the displacements for the heave and pitch [12]. These displacements are applied in a rigid body fashion and the grid is updated. The velocity of the grid is applied from one time step to the next one by dividing the time step size in different positions. This process is repeated for several time steps. Then the velocity of the grid is extracted in the Navier-Stokes Equation to account and simulate deck movement by a dynamic mesh technique. This can be done by secondary development of Ansys Fluent which program code is embedded in it by the user defined function (UDF). Simulations of wind speed ends if the displacement divergent or decaying is observed. The critical velocity of flutter is found by plotting the time history of the structure motion induced response.

ISSN 2349-4506
Impact Factor: 2.265

Global Journal of Engineering Science and Research Management

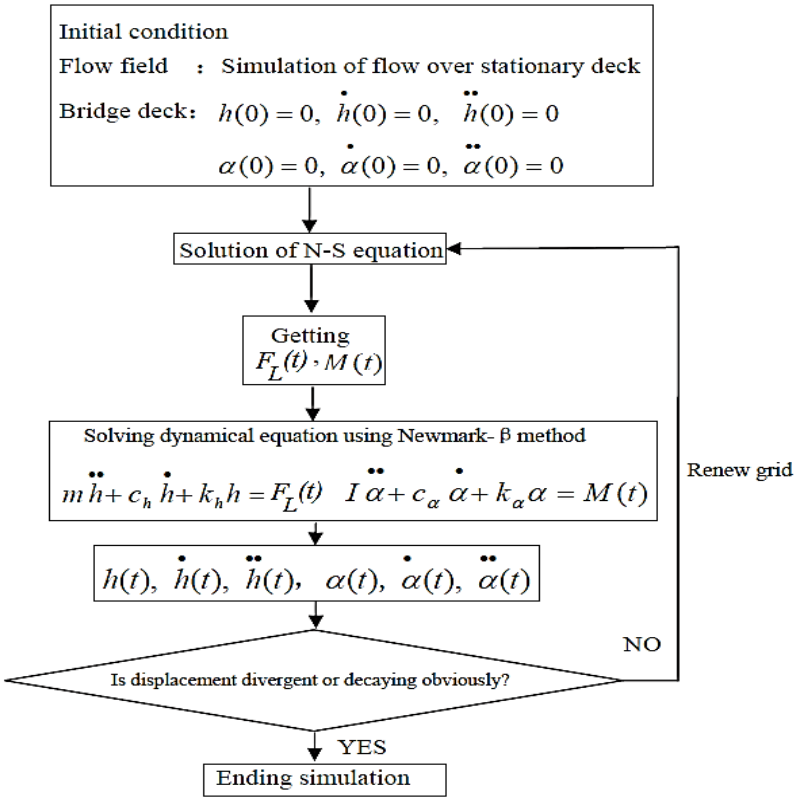

Fig. 4: Procedure of FSI in every wind speed [9]

CFD methodology for both steady and unsteady simulations is shown in Fig.5. A 2D analyzed section has been modeled by the incompressible turbulence of the Navier-Stokes Equation. The simulations employed by realizable (κ-ε) model with enhanced wall treatment.

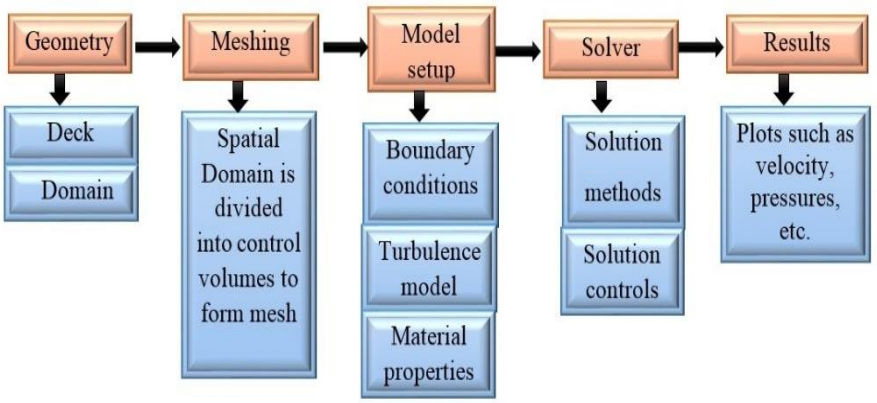

Fig.5: Flow chart for "CFD methodology" over bridge deck [13]

At the inlet and outlet boundaries Dirichlet conditions have been committed; however at deck sections surface no-slip conditions have been imposed. The turbulent flow characteristics has been defined with respect to the intensity

and viscosity ratio. For the pressure-velocity a coupling implicit scheme for second-order and PISO algorithm are used. It is found that the PISO scheme for pressure-velocity coupling provides faster convergence for transient flow than the standard SIMPLE approach [11, 14].

Flutter derivative

In classical approach for the flutter problems the self-excited forces is a mix of frequency and time domain analysis by using flutter derivatives equations (8),(9) and (10).The aerodynamic forces are determined from the flutter derivatives which usually extracted from sectional model tests in a wind tunnel, using numerous techniques from either free or forced oscillation experiments. The Discrete Vortex Method (DVM) has been used to derive the flutter derivatives according to the model by Simiu and Scanlan [7].These aerodynamic forces per unit span are related to the sway, heave and torsional displacements of the bridge deck, as denoted by *p*, *h*, α and the associated velocity $\dot{p}$, $\dot{h}$, $\dot{\alpha}$ which can be expressed as follow:

$$F_D = \frac{1}{2}\rho U^2 B[KP_1^*\frac{p}{U} + KP_2^*\frac{B\dot{\alpha}}{U} + K^2P_3^*\alpha + K^2P_4^*\frac{p}{B} + KP_5^*\frac{h}{U} + K^2P_6^*\frac{h}{B}] \quad (8)$$

$$F_L = \frac{1}{2}\rho U^2 B[KH_1^*\frac{\dot{h}}{U} + KH_2^*\frac{B\dot{\alpha}}{U} + K^2H_3^*\alpha + K^2H_4^*\frac{h}{B} + KH_5^*\frac{\dot{p}}{U} + K^2H_6^*\frac{p}{B}] \quad (9)$$

$$F_M = \frac{1}{2}\rho U^2 B[KA_1^*\frac{h}{U} + KA_2^*\frac{B\dot{\alpha}}{U} + K^2A_3^*\alpha + K^2A_4^*\frac{h}{B} + KA_5^*\frac{p}{U} + K^2A_6^*\frac{p}{B}] \quad (10)$$

In order to solve the critic flutter condition it is convenient to rewrite the equations of motion in the following forms:

$$m_p(\ddot{p} + 2\zeta_p\omega_p\dot{p} + \omega_p^2 p) = F_D \quad (11)$$

$$m_h(\ddot{h} + 2\zeta_h\omega_h\dot{h} + \omega_h^2 h) = F_L \quad (12)$$

$$I(\ddot{\alpha} + 2\zeta_\alpha\omega_\alpha\dot{\alpha} + \omega_\alpha^2\alpha) = F_M \quad (13)$$

By substituting equations (11) to (13) into equations (8) to (10) the classic flutter equations can be simplified as follow:

$$m_p(\ddot{p} + 2\zeta_p\omega_p\dot{p} + \omega_p^2 p) = \frac{1}{2}\rho U^2 B[KP_1^*\frac{p}{U} + KP_2^*\frac{B\dot{\alpha}}{U} + K^2P_3^*\alpha + K^2P_4^*\frac{p}{B} + KP_5^*\frac{h}{U} + K^2P_6^*\frac{h}{B}] \quad (14)$$

$$m_h(\ddot{h} + 2\zeta_h\omega_h\dot{h} + \omega_h^2 h) = \frac{1}{2}\rho U^2 B[KH_1^*\frac{\dot{h}}{U} + KH_2^*\frac{B\dot{\alpha}}{U} + K^2H_3^*\alpha + K^2H_4^*\frac{h}{B} + KH_5^*\frac{\dot{p}}{U} + K^2H_6^*\frac{p}{B}] \quad (15)$$

$$I(\ddot{\alpha} + 2\zeta_\alpha\omega_\alpha\dot{\alpha} + \omega_\alpha^2\alpha) = \frac{1}{2}\rho U^2 B[KA_1^*\frac{h}{U} + KA_2^*\frac{B\dot{\alpha}}{U} + K^2A_3^*\alpha + K^2A_4^*\frac{h}{B} + KA_5^*\frac{p}{U} + K^2A_6^*\frac{p}{B}] \quad (16)$$

Where:

K: Reduced frequency K= Bω/U.

ω :Circular frequency.

H_i^*, P_i^*, A_i^* (i =1 to 6): Dimensionless flutter derivatives determined experimentally from wind tunnel tests.

ζ_p, ζ_h, ζ_α: Damping ratios for the sway, heave and torsional motions respectively.

ω_p,ω_h, ω_α: Natural circular frequencies of the sway, heave and torsional motions respectively.

Based on equations (14) to (16), three-degree coupling flutter analysis method can be proposed to determine the critical wind speed of flutter. However since the number of aerodynamic flutter derivatives is eighteen, six for each mode of motion. It is much more difficult to obtain all the values through wind tunnel experiments. As a result the simplified two dimensional DVM by forcing sinusoidal motion at non dimensional wind speeds with only 8 flutter derivatives equations (17) and (18) is still very popular for bridge wind tunnel experiments.

$$m_h(\ddot{h} + 2\zeta_h\omega_h\dot{h} + \omega_h^2 h) = \frac{1}{2}\rho U^2 B[KH_1^*\frac{\dot{h}}{U} + KH_2^*\frac{B\dot{\alpha}}{U} + K^2H_3^*\alpha + K^2H_4^*\frac{h}{B}] \quad (17)$$

$$I(\ddot{\alpha} + 2\zeta_\alpha\omega_\alpha\dot{\alpha} + \omega_\alpha^2\alpha) = \frac{1}{2}\rho U^2 B[KA_1^*\frac{h}{U} + KA_2^*\frac{B\dot{\alpha}}{U} + K^2A_3^*\alpha + K^2A_4^*\frac{h}{B} \quad (18)$$

ISSN 2349-4506
Impact Factor: 2.265

Global Journal of Engineering Science and Research Management

The formulas for the determination of the eight flutter derivatives are as flow:

$$H_1^* = -\left(\frac{U}{fB}\right)^2 \frac{C_L \sin\varphi}{2(2\pi)^2 (h/B)} \qquad A_1^* = -\left(\frac{U}{fB}\right)^2 \frac{C_M \sin\varphi}{2(2\pi)^2 (h/B)}$$
$$H_2^* = -\left(\frac{U}{fB}\right)^2 \frac{C_L \sin\varphi}{2(2\pi)^2 \alpha} \qquad A_2^* = -\left(\frac{U}{fB}\right)^2 \frac{C_M \sin\varphi}{2(2\pi)^2 \alpha} \qquad (19)$$
$$H_3^* = \left(\frac{U}{fB}\right)^2 \frac{C_L \cos\varphi}{2(2\pi)^2 \alpha} \qquad A_3^* = \left(\frac{U}{fB}\right)^2 \frac{C_M \cos\varphi}{2(2\pi)^2 \alpha}$$
$$H_4^* = \left(\frac{U}{fB}\right)^2 \frac{C_L \cos\varphi}{2(2\pi)^2 (h/B)} \qquad A_4^* = \left(\frac{U}{fB}\right)^2 \frac{C_M \cos\varphi}{2(2\pi)^2 (h/B)}$$

If a harmonic motion of the bridge is assumed to be as in equations (20) and (21):

$$h(t) = h_0 e^{i\omega t} = h_0 e^{iKs} \qquad (20)$$
$$\alpha(t) = \alpha_0 e^{i\omega t} = \alpha_0 e^{iKs} \qquad (21)$$

Where:
S: convenient non-dimensional time s= Ut /B

By substituting equations (20) and (21) into the flutter equations (17) and (18) it led to equations (22) and (23)

$$\frac{h_0}{B}\left[-K^2 + 2\zeta_h K_h Ki + K_h^2 - \frac{\rho B^2}{m} K^2 H_1^*(K) i - \frac{\rho B^2}{m} K^2 H_4^*(K)\right] - \alpha_0\left[\frac{\rho B^2}{m} K^2 H_2^*(K) i + \frac{\rho B^2}{m} K^2 H_3^*(K)\right] = 0$$
$$\frac{h_0}{B}\left[\frac{\rho B^4}{I} K^2 A_1^*(K) i - \frac{\rho B^4}{I} K^2 A_4^*(K)\right] + \alpha_0\left[-K^2 + 2\zeta_\alpha K_\alpha Ki + K_\alpha^2 - \frac{\rho B^4}{I} K^2 A_2^*(K) i - \frac{\rho B^4}{I} K^2 A_3^*(K)\right] = 0$$

(22)

(23)

By defining the unknown (X) as in equation (24) and setting the determinant of the coefficients of h and α in equation (20) and (21) to be zero, the results are a fourth order complex polynomial in (X), the real and imaginary parts are shown in equations (25) and (26).The solution for the unknown flutter frequency (ω), will be in the form $\omega = \omega_1 + i\omega_2$ and will represent either a decaying ($\omega_2 > 0$) or a divergent ($\omega_2 < 0$) oscillation. The critical flutter condition can be found when $\omega_2 = 0$, so that $\omega = \omega_1$. The two quartic polynomials in equations (25) and (26) are solved at different values of frequency and the roots of the real and imaginary parts are plotted against reduced velocity (V*) which shown in equation (27).

$$X = \frac{\omega}{\omega_h} \qquad (24)$$

$$R_4 X^4 + R_3 X^3 + R_2 X^2 + R_1 X + \frac{K_\alpha^2}{K_h^2} = 0 \qquad (25) \qquad \text{Real}$$

$$I_4 X^4 + I_3 X^3 + I_2 X^2 + I_1 X = 0 \qquad (26) \qquad \text{Imaginary}$$

Where:

Global Journal of Engineering Science and Research Management

$$R_4 = 1 + \frac{\rho B^4}{I} A_3^* + \frac{\rho B^2}{m} H_4^* - \frac{\rho^2 B^6}{mI} H_1^* A_2^* + \frac{\rho^2 B^6}{mI} A_3^* H_4^* + \frac{\rho^2 B^6}{mI} A_1^* H_2^* - \frac{\rho^2 B^6}{mI} H_3^* A_4^*$$

$$R_3 = 2\zeta_h \frac{\rho B^4}{I} A_2^* + 2\zeta_\alpha \frac{\rho B^2}{m} \frac{K_\alpha}{K_h} H_1^*$$

$$R_2 = -\frac{K_\alpha^2}{K_h^2} - 4\zeta_h \zeta_\alpha \frac{K_\alpha}{K_h} - 1 - \frac{\rho B^4}{I} A_3^* - \frac{\rho B^2}{m} \frac{K_\alpha^2}{K_h^2} H_4^*$$

$$R_1 = 0$$

$$I_4 = \frac{\rho B^4}{I} A_2^* + \frac{\rho B^2}{m} H_1^* + \frac{\rho^2 B^6}{mI} A_3^* H_1^* + \frac{\rho^2 B^6}{mI} A_2^* H_4^* - \frac{\rho^2 B^6}{mI} A_4^* H_2^* - \frac{\rho^2 B^6}{mI} A_1^* H_3^*$$

$$I_3 = -2\zeta_\alpha \frac{K_\alpha}{K_h} - 2\zeta_h - 2\zeta_h \frac{\rho B^4}{I} A_3^* - 2\zeta_\alpha \frac{\rho B^2}{m} \frac{K_\alpha}{K_h} H_4^*$$

$$I_2 = -\frac{\rho B^4}{I} A_2^* - \frac{\rho B^2}{m} \frac{K_\alpha^2}{K_h^2} H_1^*$$

$$I_1 = 2\zeta_h \frac{K_\alpha^2}{K_h^2} + 2\zeta_\alpha \frac{K_\alpha}{K_h}$$

$$V^* = \frac{V_0}{fB} \qquad (27)$$

The point at which the roots of the two equations cross, (V*, X_c) defines the flutter condition [7]. This gives the frequency of the flutter instability (ω) and combined with appropriate structural parameters, the critical flutter velocity can be found from equation (28)

$$V_{Cr} = \frac{V^* \omega_h B X_C}{2\pi} \qquad (28)$$

In wind engineering, the derivatives A_4* and H_4* are assumed to be zero as they give little significance for practical flutter predictions [6]. The DVM analysis for critical wind speed of flutter results are presented for two cases, the first using only the traditional derivatives A_i* and H_i* for i=1-3 and the second also including the two derivatives, A_4* and H_4* to study its influence in results.

Modal Analysis

Ansys is a finite element program that can calculate the natural frequencies and mode shapes of a structure. To calculate natural frequencies and modes, Ansys can use eigensolver. This is a method that iterates the eigenvalue problem until the solution is obtained as shown in equation (29)

$$(\boldsymbol{K} - \omega_j^2 \boldsymbol{M})\varphi_j = 0 \qquad (29)$$

Where:

K: The stiffness matrix.
M**:** The mass matrix.
ω_j :Natural frequency.
ϕ_j :The associated eigenvector.

Ansys can calculate as many natural frequencies as there are many degrees of freedom (DOF) in the model. It is possible to specify the number of desired natural frequencies to calculate. The mode shapes at high frequencies are not interesting so it is normal to only look at the first frequencies of lateral, vertical and torsional. Equation (29) shows that the stiffness matrix and mass matrix are those that determine the natural frequencies and modes. So the important thing when modeling a bridge in Ansys is to represent the mass and stiffness properties correct.

Numerical Simulation Model of the Great Belt East Bridge

ISSN 2349-4506
Impact Factor: 2.265

Global Journal of Engineering Science and Research Management

In this section, numerical simulations of the wind action on a cross section that belongs to the Great Belt East Bridge are presented, including the aerodynamic and the aeroelastic behavior. The studies are accomplished by fixed and oscillating sectional models, according to the usual wind tunnel techniques. The Great Belt East Bridge as shown in Fig.6 is one of the longest suspension bridges located in Denmark precisely in the Great Belt Channel, an important international shipping route. The design phase was initiated in 1989, being opened to the traffic in 1998. The central span equals 1624 m and side span of 535 m. The bridge deck is 31 m wide and 4.4 m deep steel box. This girder is continuous over the full cable supported length of 2694 m. The form of the box girder is streamlined to resist the aerodynamic instability due to the strong wind. The ratio of cable sag to main span length is 1/9. The main cables are fixed through stiffening girder at the mid span. The total height of the concrete pylons is 258 m. The bridge geometries are shown in Fig.7 and its properties which are used in aerodynamic coefficients, flutter analysis and modal analysis are given in Table 1 and Table 2.

Fig. 6: Great Belt Suspension Bridge

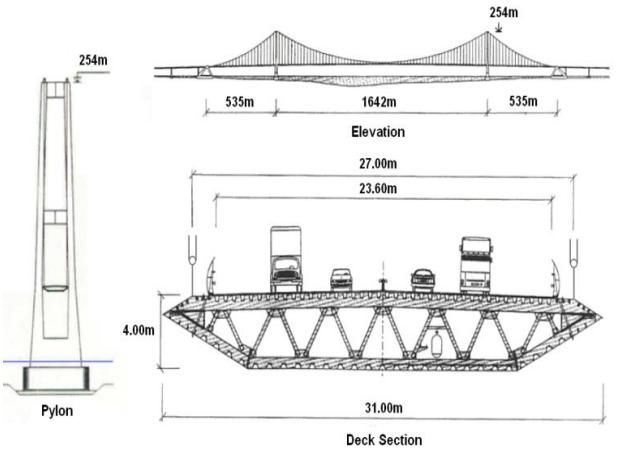

Fig.7: Dimensions of the Great Belt Suspension Bridge (Elevation, Deck section and Pylon) [15]

For CFD analysis the height of the fluid domain is10 B and the length is16 B where (B) is the deck width. Fig.8 shows the domain regions and dimensions. Rigid mesh grid is used in the inner region while stationary mesh grid is used in the outer region. Dynamic mesh grid is between the rigid mesh and stationary mesh. The width and height of the rigid mesh are about two times and one times the width of the deck section respectively. Both the width and height of the dynamic mesh grid are about six times the width of the deck section.

When the deck section vibrates, the rigid mesh grid follows the deck section synchronously. The static grid stays stationary while the shape and dimension of the dynamic mesh changes constantly. In the region which is far away from the deck section, the size of the mesh grid is big. On the contrary, in the region which is near the deck section the mesh grid is small.

The boundaries of the domain flow are considered as the flow runs from the left to the right. The left side is considered as the inflow boundary specified with the velocity inlet. On the other right side there is an exit boundary specified with pressure outlet equal to zero. The upper and lower sides are specified as symmetrical. The deck edges are considered as a wall with no-slip boundary conditions.

The mesh information and size are defined by the number of cells, nodes, and faces. Fig.9 and Table 3 show the definition of them. The whole numerical grids of the deck section is shown in Fig.10.

Table 1. Structural data used in the flutter analysis [16]

Parameters	Units	Values

ISSN 2349-4506
Impact Factor: 2.265
Global Journal of Engineering Science and Research Management

Natural vertical frequency (f_v)	Hz	0.099
Natural torsional frequency (f_t)	Hz	0.272
Mass per unit length (m)	kg/m	23687
Mass moment of inertia about shear center per unit length (I)	$Kg.m^2/m$	2.501×10^6
Equivalent spring stiffness for vertical bending mode per unit length (K_h)	Kg/m^2	878.506
Equivalent spring stiffness for torsional mode per unit length (K_α)	Kg.m/m	7.194×10^5

Table 2. Geometries and material properties used for modal analysis [17]

Member	E (GPa)	A (m^2)	I (m^4)	W (KN/m)
Deck	210	1	3.32	144.8
Main span cable	210	0.40	-	32.9
Side span cable	210	0.41	-	33.8
Hanger	210	0.025	-	-
Pylon (0-75.5 m)	40	37.5	750	882.4
Pylon (75.5-136.2 m)	40	32.5	275	764.4
Pylon (136.2-196.9 m)	40	30.0	200	705.6
Pylon (196.9-257.6 m)	40	25.0	150	588.0

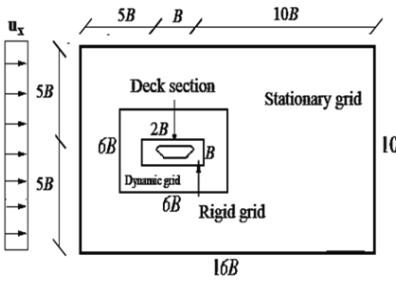

Fig.8: Domain regions and dimensions

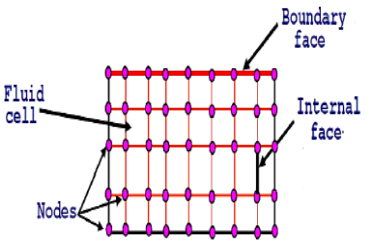

Fig.9: Definition of cells, nodes, and face [12]

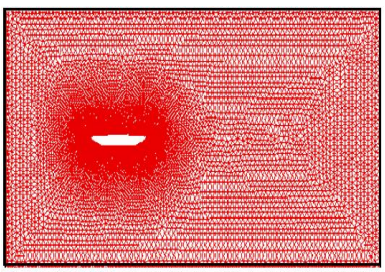

Fig.10: Whole mesh for deck section

Table 3 .Mesh information for studied deck section (CFD-Model)

Definition	Cells	Nodes	Faces
Number	97360	53996	151356

The time step was equal to 0.001 in the transient state simulations for (t*) equal to 60 seconds and the number of iterations per each time step was 10. Unsteady simulations continued until a periodic behavior was reached. Computations have been carried out on core i7, 2.10 GHz and physical memory 8.00 GB.

According to the bridge design, the initial FEM of the Great Belt East Bridge was established based on ANSYS 14.5, as shown in Fig. 11.In the FEM, the main girders and towers were modeled by spatial beam elements with 6 DOF at each node. The element stiffness was taken as its actual stiffness. The tower columns were divided into 40 elements, the higher and lower cross beams of the towers were all divided into 12 elements. The main cable and the suspender were simulated spatial truss elements with 3 DOF at each node .The suspension cables are connected to the girder through rigid link elements every 24 m by pair of hangers and the main cable was also

meshed to match the nodes of the suspender. The main span of the bridge is discretized into 112 frame elements and the damping ratio is assumed as 0.5% .

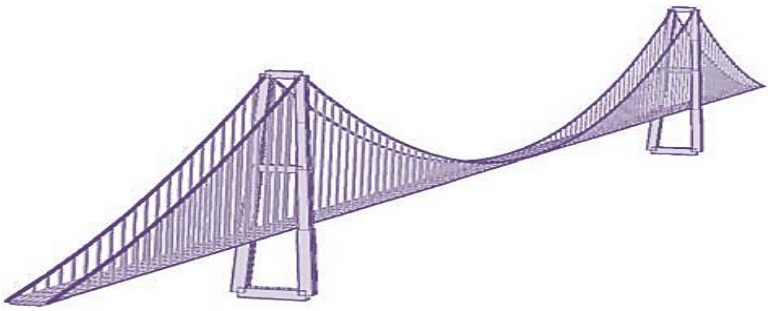

Fig.11: Finite element model of The Great Belt Bridge.

NUMERICAL SIMULATION RESULTS

Steady Aerodynamic Force Coefficients

In order to validate the cross sectional geometry adopted for suspension bridges, the finite volume grid and the 2D approach in the CFD analysis for the deck are used. Static aerodynamic coefficients have been computed assuming steady state. The aerodynamic coefficients have been computed for Reynolds number equal to 10^5 based on the deck width with different angles of attack in the range of -10º to 10º with step 2º.

In the studied (k-ε) turbulence model the second order scheme was used. The number of chosen iterations was 2000 in steady state simulations. In Fig.12 the computed static aerodynamic force coefficients are presented along with the experimental results obtained by Walther and Reinhold [18, 19] for the same Reynolds number. The computational results are in good agreement with those obtained by other researchers.

Unsteady Time History of Aerodynamic Coefficients

Direct Method

To find the critical wind speed of flutter for the deck cross section, time history analysis for aerodynamic coefficients and vibrating motion should be applied by increasing the inlet velocity incrementally in different runs [12]. When the aerodynamic coefficients and motion amplitude started to grow (negative damping), the critical velocity was found [12]. From Fig.s 13 and 14 it can be seen that:

- When wind speed equals 68 m/sec, lift and moment coefficients decrease with the increase of time. This illustrates that the total damping of the model is positive.
- When wind speed equals 69 m/sec, lift and moment coefficients remain almost the same.
- When wind speed reaches 70 m/sec, lift and moment coefficients increase with the increase of time. This illustrates that the total damping of the model changes from positive to negative. So flutter critical wind speed equals 70 m/sec.
- When flutter occurs, the torsional vibration frequency equals 0.2 Hz. Comparing this frequency with fv and ft shown in Table 1, the flutter style for deck section is bending torsional coupled flutter.

Flutter Derivative Method

The DVM has been used to derive the flutter derivatives for the Great Belt bridge deck from a series of calculations of the section undergoing forced sinusoidal oscillations. The simulations involved separate vertical and torsional motion. The deck was analyzed for fifth reduced velocities: 2.5,5, 10, 12.5 and 15. These values correspond to equation (27) and fv led to inflow velocities: 21.08 m/s, 42.16 m/s, 63.24 m/s, 84.32 m/s, 105.4 m/sec and 126.48 m/sec, respectively. The flow was analyzed with Re = 10^5. The amplitudes were 4%B and 4° for the vertical and torsional cases respectively.

The DVM results are presented for two cases, the first using only the traditional derivatives A_i and H_i for i=1-3 and the second also including the two derivatives, A_4* and H_4*.The flutter derivatives were extracted from the

ISSN 2349-4506
Impact Factor: 2.265

Global Journal of Engineering Science and Research Management

DVM are compared with those from [15] as in Fig.15.

In Fig. 16, time history related to the torsional displacement (α_t) is presented for selected reduced wind velocity. It can be seen that the torsional displacement decrease with the increase of time for reduced wind velocity from 2.5 m/sec to 10 m/sec. This illustrates that the total damping of the model is still positive. On the contrary the torsional displacement increase with the increase of time when the reduced wind velocity equals 12 m/sec. This illustrates that the total damping of the model changes from positive to negative. So flutter critical wind speed Vcr is between (10 -12.5) m/sec.

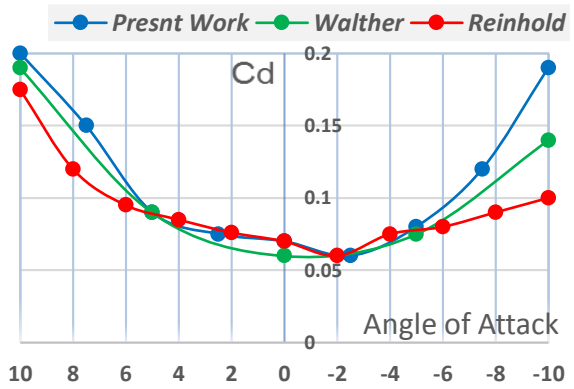

(a) Drag coefficient (C_d)

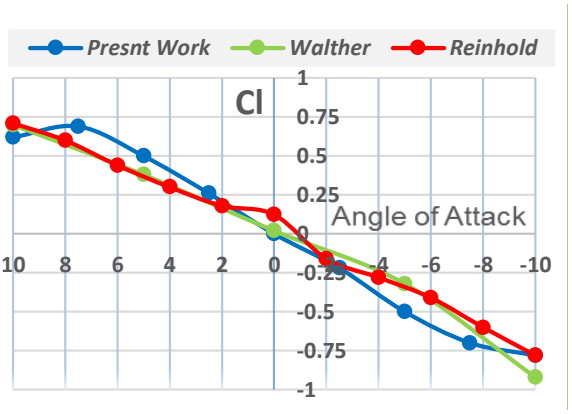

(b) Lift coefficient (C_l)

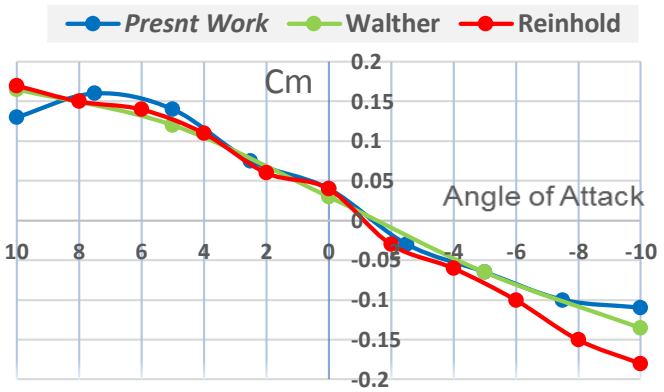

(C) Moment coefficient (C_m)

Fig.12: Aerodynamic coefficients for Re=10^5.

ISSN 2349-4506
Impact Factor: 2.265

Global Journal of Engineering Science and Research Management

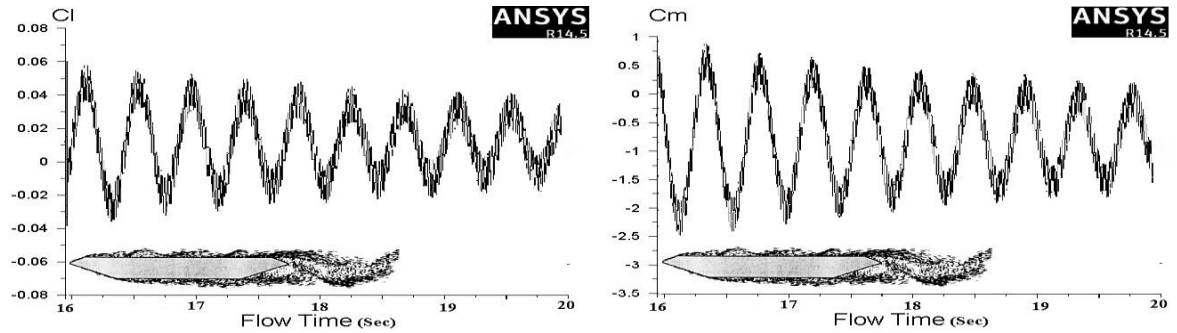

a) V= 68 m/sec

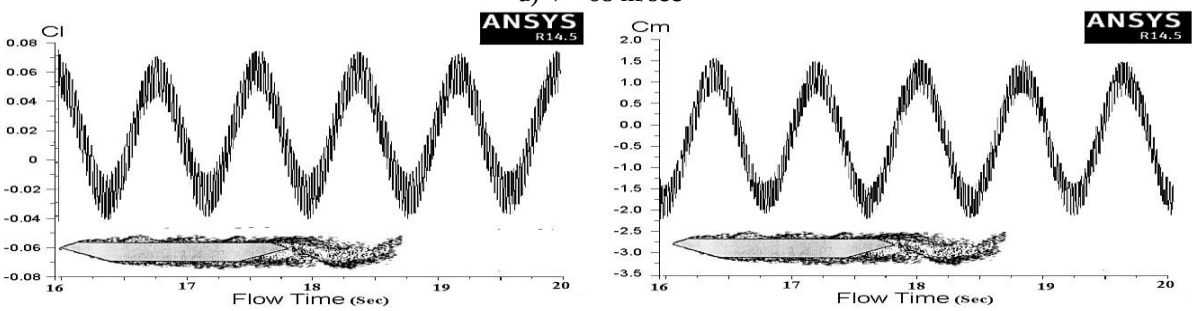

b) V= 69 m/sec

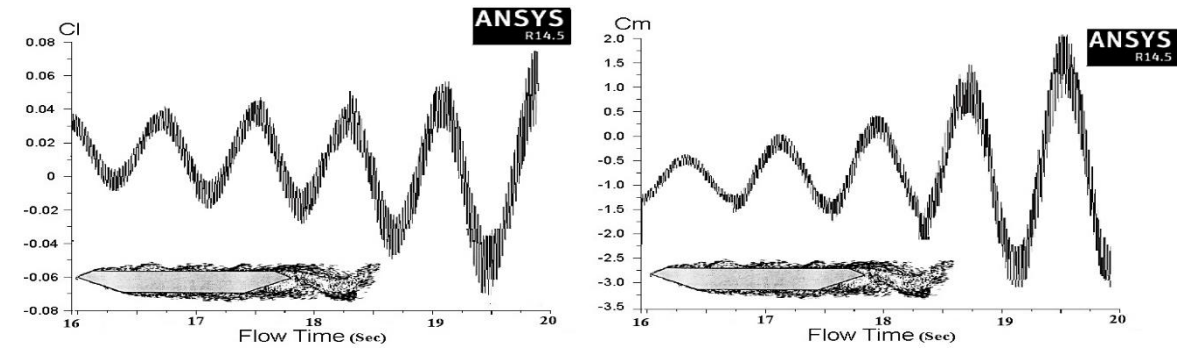

c) V= 70 m/sec

Fig.13 Time histories of lift and moment coefficients.

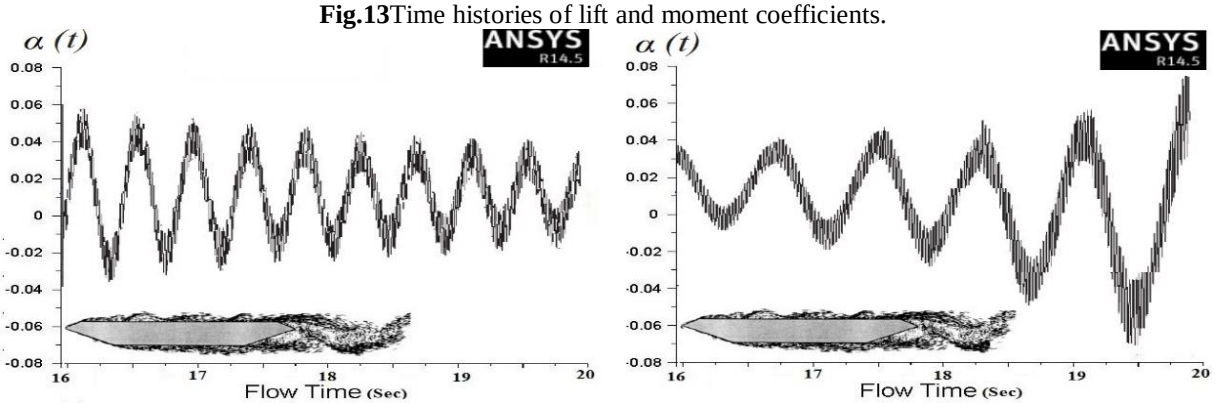

(a) V=68 m/sec (b) V=70 m/sec

Fig.14 Time histories of torsional displacement for deck section (1)

ISSN 2349-4506
Impact Factor: 2.265
Global Journal of Engineering Science and Research Management

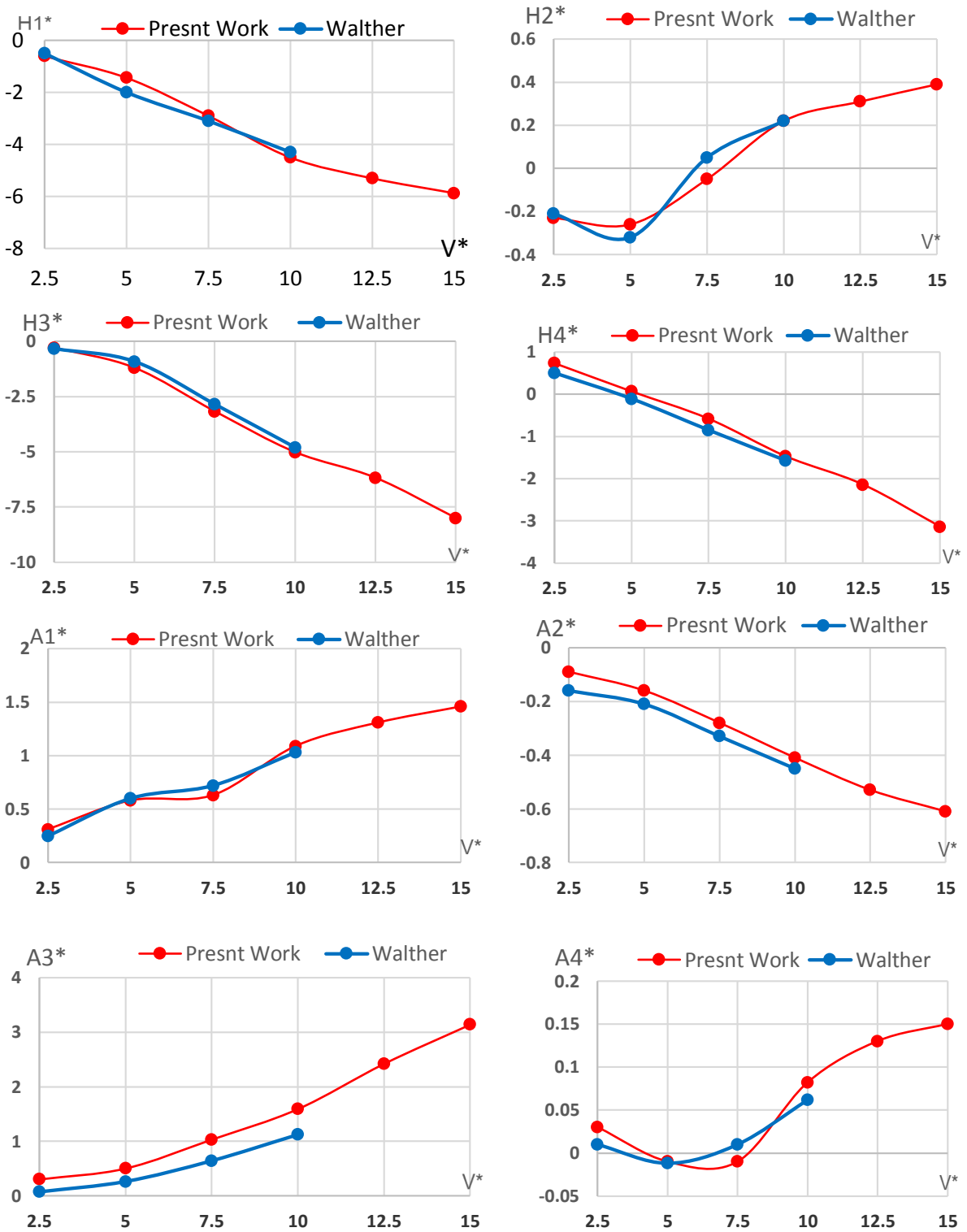

Fig.15: Flutter derivatives comparison as a function of the reduced velocity

ISSN 2349-4506
Impact Factor: 2.265

Global Journal of Engineering Science and Research Management

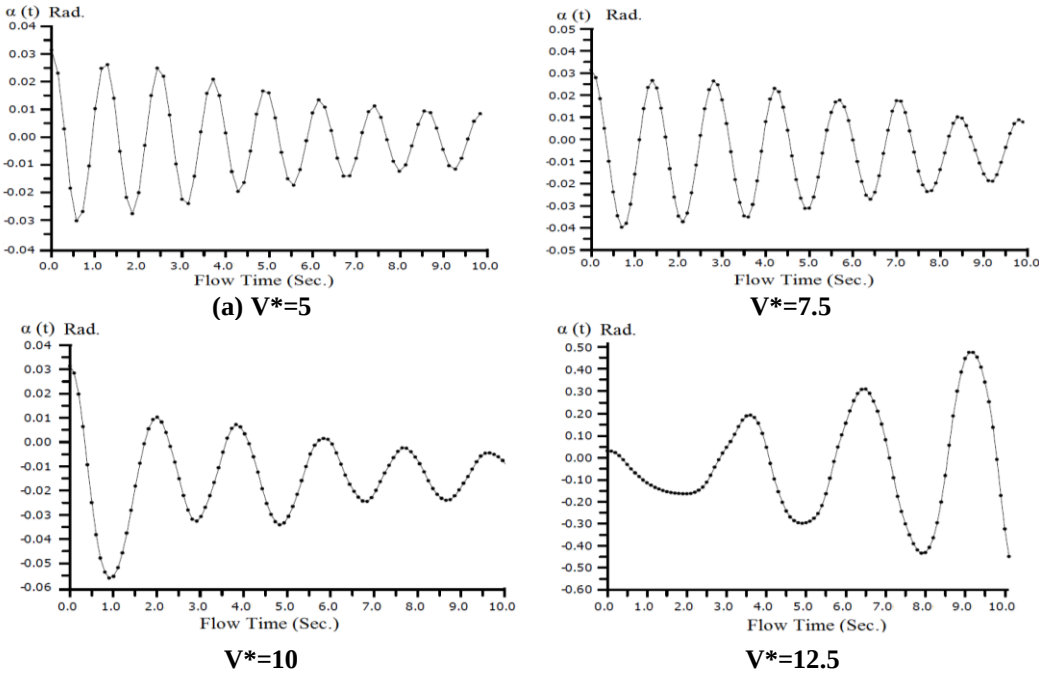

Fig.16: Time history analysis related to the angular displacement (α t) for selected reduced velocity (V*)

To get the exact value of Vcr the two quartic polynomials equation (25) and (26) are solved at different values of reduced velocity V* and the roots of the real and imaginary parts are plotted against *(X)*.The point at which the roots of the two equations cross, (V*, X_c) defines the flutter condition .This gives the frequency of the flutter instability (ω).

The point of intersection between the two equations roots is (11.162, 2.125) for DVM A_i* and H_i*where i=1-4 Fig.17 and (12.394, 1.967) for DVM A_i* and H_i*where i=1-3 only Fig.18.Now critical wind speed of flutter can be determined for the two cases by using equation (28) and the frequency of the flutter (ω) can be determined from equation (24),Then comparing this frequency with fv and ft to know the flutter style for the deck section as flow.

$$\omega_h = 2\pi f = 2 * 3.142 * 0.099 = 0.622\, rad/sec$$

For (DVM –A_i* and H_i*, where i=1-4)

$$V_{Cr} = \frac{V^* \omega_h B X_C}{2\pi} = \frac{11.162 * 0.622 * 31 * 2.125}{2 * 3.142} \longrightarrow V_{Cr} = 72.79\, m/sec$$

$$\omega = X * \omega_h = 2.125 * 0.622 \longrightarrow \omega = 1.322\, rad/sec$$

$$f = \frac{\omega_h}{2\pi} = \frac{1.322}{2*3.142} \longrightarrow f = 0.210\, Hz$$

For (DVM –A_i* and H_i*, where i=1-3 only)

$$V_{Cr} = \frac{V^* \omega_h B X_C}{2\pi} = \frac{12.394 * 0.622 * 31 * 1.967}{2 * 3.142} \longrightarrow V_{Cr} = 74.81\, m/sec$$

$$\longrightarrow$$

ISSN 2349-4506
Impact Factor: 2.265

Global Journal of Engineering Science and Research Management

$$\omega = X * \omega_h = 1.967 * 0.622 \qquad \omega = 1.223\ rad/sec$$

$$f = \frac{\omega_h}{2\pi} = \frac{1.223}{2 * 3.142} \longrightarrow f = 0.193\ Hz$$

The previous two frequencies values are between fv= 0.097 Hz and ft =0.272 this means that the flutter style for this deck section is bending torsional coupled flutter.

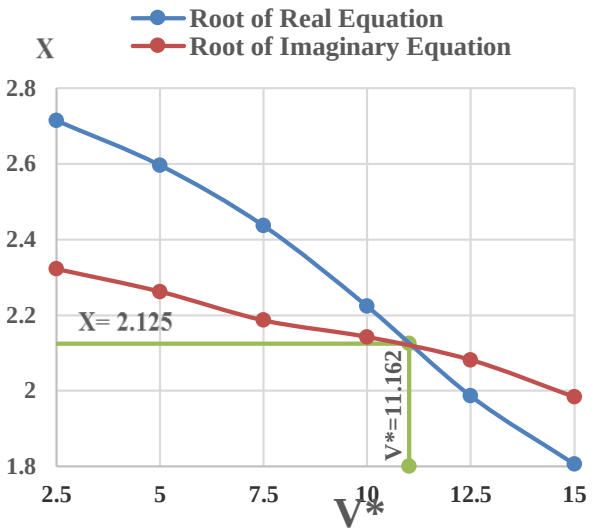

Fig.17: Solution of flutter equations to get critical flutter velocity in case Ai and Hi*, where i=1-4.*

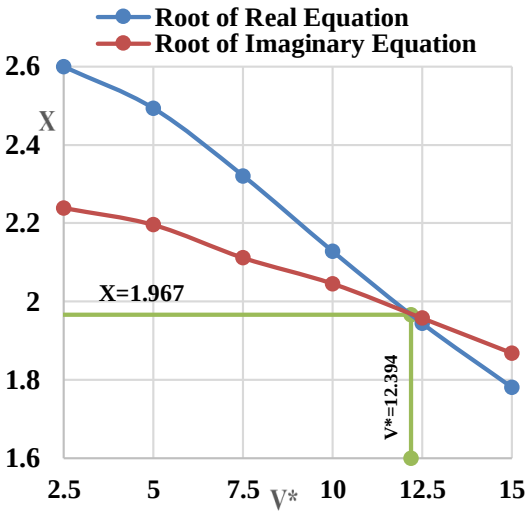

Fig.18; Solution of flutter equations to get critical flutter velocity in case A_i and H_i*, where i=1-3 only.*

Modal Analysis

The first, second and third fundamental mode of the lateral, vertical and torsional are shown in Fig.19.

Comparison of Results

Steady simulations of the deck configuration considering Reynolds number equals 10^5 and range of angles of attack have offered aerodynamic coefficients close to those obtained from Walther and Reinhold [18, 19] for the same Reynolds number as shown in Fig.12.

Flutter velocity predictions from the FSI and DVM analysis are presented in Table 4 compared with results obtained from other researchers. The FSI and DVM methods give an excellent prediction of the critical flutter velocity. The accuracy of these methods are useful analysis tool for design studies of long span bridges.

The results of the frequencies values are relatively accurate comparing to the corresponding experimental and numerical values given in Table 5.

ISSN 2349-4506
Impact Factor: 2.265

Global Journal of Engineering Science and Research Management

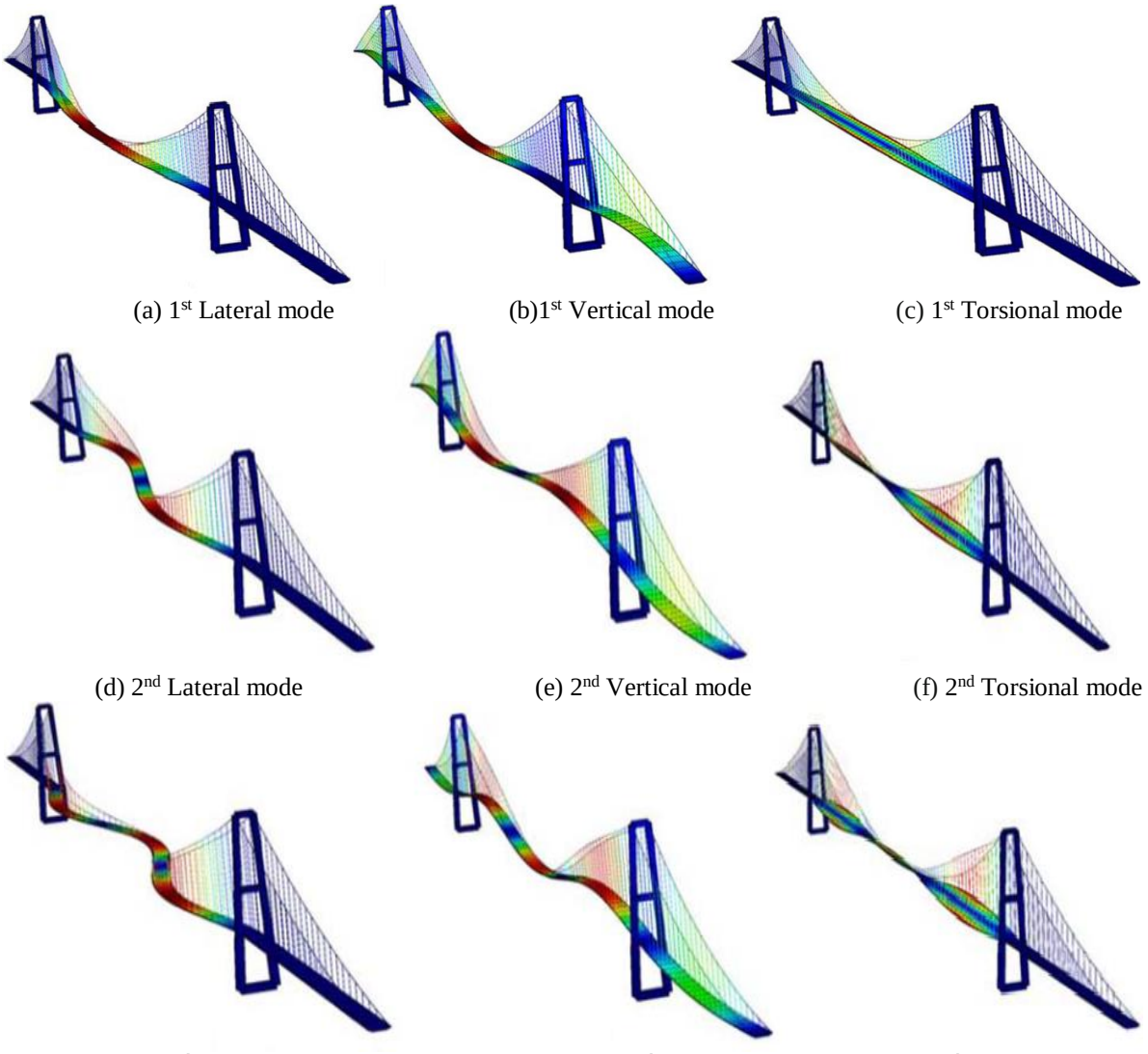

(a) 1st Lateral mode (b)1st Vertical mode (c) 1st Torsional mode

(d) 2nd Lateral mode (e) 2nd Vertical mode (f) 2nd Torsional mode

(g) 3rd Lateral mode (h) 3rd Vertical mode (i) 3rd t Torsional mode

Fig.19: Frist, Second and Thread Modes of the lateral, vertical and torsional of the Great Belt Bridge.

Table 4. References of flutter velocity for the Great Belt East Bridge.

Reference	**Vcr (m/s)**
(FSI with CFD) Present work	70
(DVM $-A_i$* and H_i* i=1-3 only) Present Work	75
(DVM- A_i* and H_i* i=1-4) Present Work	72.79
(DVM $-A_i$* and H_i* i=1-3 only) Robert and Kenneth [11]	71.9
(FSI with CFD) Hao Zhan [1]	69
(Wind Tunnel Tests) Hao Zhan [16]	73
Vortex method Larsen [20]	74
Taut strip (Experimental) Larsen, A. & Walther, J. H [15]	72

Table 4. Modal analysis results

Global Journal of Engineering Science and Research Management

Mode Shape Description	Frequency(Hz)		
	Present Work	Analytical	Experimental
		Larsen [20]	Larsen and Jacobsen [21]
1st Lateral	0.059	0.052	0.0523
2nd Lateral	0.141	0.123	0.127
3ed Lateral	0.246	0.187	
1st Vertical	0.106	0.100	0.997
2nd Vertical	0.115	0.115	0.115
3rd Vertical	0.132	0.135	
1st Torsional	0.310	0.278	0.289
2nd Torsional	0.414	0.383	0.391
3rd Torsional	0.542	0.502	

CONCLUSIONS

The following points offer the major outcome of the present study:

1) The computational two methods FSI and DVM can lead to a reduction in the number of expensive physical model tests .It should be recognized that the CFD method is a time and cost-saving approach to identify critical wind speed of flutter for long span bridges.
2) Steady CFD simulation curves of the aerodynamic coefficients have been evaluated for a wide range of angles of attack and the computed results showed acceptable agreement between experimental results and simulation results for the same Reynolds number.
3) Unsteady 2D simulations of time history analysis for aerodynamic coefficients led to find the critical wind speed of flutter by increasing the inlet velocity incrementally in different runs. When the aerodynamic coefficient and motion amplitude started growing (negative damping), the critical wind speed was found.
4) FSI is considered as a direct simulation method for the flutter stability of bridge deck and was developed based on CFD software Ansys Fluent and proved to be useful in the early aerodynamic design stage of long span suspension bridges.
5) The flutter derivatives were calculated for the deck cross section and compared with the results in another references a good agreement was found for these simulation results.
6) The DVM results are presented for two cases, the first using only the traditional flutter derivatives Ai* and Hi* for i=1-3 and the second also including the two derivatives, A4* and H4*. The DVM predictions give an excellent prediction of the critical flutter velocity. The accuracy of these results indicates that the DVM is a useful analysis tool for design studies of long span bridges.
7) In the near future fluid-structure interaction (FSI) based on computational fluid dynamics (CFD) will be used in studying complex geometry decks of suspension bridges considering details such as guardrails, cables and aerodynamic appendages. Refinements in processing time and semi-implicit schemes can also be expected

REFERENCES

1. Hao Zhan ,Tao Fang ,Zhiguo Zhang,"Flutter stability studies of Great Belt East suspension bridge by two CFD numerical simulation methods", 6th European & African Conference on Wind Engineering, Robinson College, Cambridge, UK, 7-11 July 2013.
2. W.M. Zhang, Y.J. Ge and M.L. Levitan," Aerodynamic flutter analysis of a new suspension bridge with double main spans", journal of Wind and Structures, Vol.14, Issue 3, 2011
3. Ding, Q., Chen, A., Xiang, H.,"Coupled flutter analysis of long-span bridges by multimode and full-order approaches", Journal of Wind Engineering and Industrial Aerodynamics Vol. 90, pp1981–1993,2002

4. Hua, X.G.,Chen,Z.Q.,Ni,Y.Q.,Ko,J.M.,.Flutter analysis of long-span bridges using ANSYS .Wind and Structure,Vol.10,Issue 1,pp61–82, 2007
5. Wang, H., Li, A.Q., Hu, R.,"Comparison of ambient vibration response of the Run yang suspension bridge under skew winds with time-domain numerical predictions. Journal of Bridge Engineering ASCE,Vol.16,Issue 4, pp 513–526, 2011
6. Selvam, R. P.; Govindaswamy, S. & Bosch, H."Aeroelastic analysis of bridges using FEM and moving grids" Wind and Structures, Vol 5, pp. 25-266, 2002.
7. Simiu E., Scanlan R.H. "Wind Effects on Structures", Third Edition., New York: John Wiley and Sons, 1996.
8. Félix Nieto, Ibuki Kusano, Santiago Hernández, JoséÁ. Jurado." CFD analysis of the vortex-shedding response of a twin-box deck cable-stayed bridge, The Fifth International Symposium on Computational Wind Engineering, Chapel Hill, North Carolina, USA, 23-27 May 2010.
9. Xiaobing Liu, Zhengqing ,and Chenb Zhiwen Liu.,"Direct simulation method for flutter stability of bridge deck", The Seventh International Colloquium on Bluff Body Aerodynamics and Applications (BBAA7),Shanghai, China; 2-6 September 2012.
10. Gergely Szabó, József Györgyi and Gergely Kristóf., Advanced flutter simulation of flexible bridge decks, Coupled Systems Mechanics, Vol. 1, Issue 2, pp. 133-154, 2012.
11. Ansys Help, Release 14.5 Documentation for Ansys, Fluid Dynamics, Ansys Fluent, Innovative turbulence modelling: in Ansys Fluent, (www.ansys.com).
12. Abdel-Aziz Ahmed, A.Attia Walid," Aeroelastic Investigation of Different Deck Sections for Suspension Bridges by Numerical Analysis" ,International Journal of Engineering and Innovative Technology (IJEIT),Vol 4, Issue 12, ,pp.49-57, June 2015.
13. Abdel-Aziz Ahmed , M. Naguib Abo El-Saad and Salah El Din El Bagalaty," Static and dynamic Analyses of suspended Cable Roofs for halls having a rectangular shape Due To Wind Loads", Mansoura Engineering Journal,Vol.35,Issue.4,pp.36-49, Dec. 2010.
14. Ashtiani Abdi, I., "Experimental and Numerical Investigation of the Wind Effects on Long Span Bridge Decks". Master's thesis, Middle East Technical University, Turkey, 2011.
15. Larsen, A. & Walther, J. H., "Aeroelastic analysis of bridge girder sections based on discrete vortex simulation", Journal of Wind Engineering and Industrial Aerodynamics, Vol. 68, pp. 253-265, 1997.
16. Hao Zhan, Tao Fang., "Flutter stability studies of Great Belt East Bridge and Tacoma Narrows Bridge by CFD numerical simulation", The Seventh International Colloquium on Bluff Body Aerodynamics and Applications (BBAA7) ,Shanghai, China; 2-6 September 2012.
17. Kim, H. K. and Lee, M. J., "Nonlinear shape-finding analysis of a self-anchored suspension bridge." Engineering Structures, 24, pp. 1547-1559, 2002.
18. Walther, J.H., "Discrete Vortex Method for Two-Dimensional Flow past Bodies of Arbitrary Shape Undergoing Prescribed Rotary and Translational Motion", PhD Thesis, Technical University of Denmark, Lyngby 1994.
19. Reinhold, T.A, Brinch, M., Damsgaard, A., "Wind tunnel tests for the Great Belt Link", Proceedings of the First International Symposium on Aerodynamics of Large Bridges, pp. 255 – 267, 1992
20. Larsen, A., "Aerodynamic aspects of the final design of the 1624 m suspension bridge across the Great Belt." J. Wind Eng. Ind Aerodyn, 48, pp. 261-285, 2003.
21. Larsen, A. and Jacobsen, S., "Aerodynamic design of the Great Belt East Bridge." Proc. First International Symposium on Aerodynamics of Large Bridges, Copenhagen, Denmark, 1992.
22. Robert Stevens and Kenneth Simonsen. Master's degree in Civil and Structural Engineering at the University of Aalborg, 2008.